[CI-12]

Sousa, J.B., **Pais, J.C.**, Stubstad, R.N.

"Mode of loading in reflective and flexural fatigue Cracking - a numeric evaluation"

Fourth International RILEM Conference and Exhibition on Reflective Cracking in Pavements, Ottawa, 2000, p. 23-35

Proceedings
PRO 11

Reflective Cracking in Pavements Research in Practice

Proceedings of the
4th International RILEM Conference

Edited by A. O. Abd El Halim,
D. A. Taylor and El H. H. Mohamed

RILEM Publications S.A.R.L.
The Publishing Company of RILEM

MODE OF LOADING IN REFLECTIVE AND FLEXURAL FATIGUE CRACKING – A NUMERIC EVALUATION

Jorge B. Sousa
Consulpav International, USA

Jorge C. Pais
University of Minho, Portugal

R. N. (Dick) Stubstad
Consulpav International, USA

Abstract

Consulpav International is working closely with the University of Minho in Portugal under a contract from the Rubber Pavements Association to develop a mechanistic procedure for overlay design that directly takes into account the mechanism of reflective cracking as well as classical flexural fatigue cracking. The problem of properly modeling the mechanism of reflective cracking is particularly prevalent in thin asphalt concrete overlays.

To correctly model and predict asphalt fatigue mechanisms in overlays (both flexural and reflective cracking), it is necessary to utilize the correct mode of loading in laboratory tests. The mode of loading chosen should, as closely as possible, reflect the mode of loading which causes crack propagation in the field

For each of the possible distress mechanisms that cause cracking in pavements, such as thin or thick existing pavement sections, and thin or thick overlays, fatigue characterization using any model must recognize that controlled stress, strain or "work" (stress x strain) will induce significantly different fatigue lives in laboratory tests. As layer moduli are reduced by fatigue mechanisms, it is necessary to investigate which of these parameters (stress, strain or work) remains mostly constant in a field situation so that it can be used as an input control parameter in laboratory fatigue tests.

This paper presents a numerical evaluation, through a finite element simulation, of mode of loading for several types of flexible pavements and overlays placed on these pavements. Stress (load), strain (displacement) and work (load x displacement) control modes are investigated.

1. Introduction

Overlay design methods that do not directly consider the phenomenon of reflective cracking may not be able to predict pavement behavior correctly. It is recognized that the use of flexural fatigue concepts prevalent in almost all of the current methods fails to capture this phenomenon. A new design method is being developed which will include criteria for the four prevailing pavement distress mechanisms, as follows:

1. *Reflective cracking* — by limiting stresses above cracks in the overlay with different limiting stress levels as a function of binder type and mix design.
2. *Tensile strain at the bottom of the overlay* — especially for thicker overlays when the neutral zone is above the bottom of the new overlay.
3. *Tensile strain at the bottom of the existing asphalt concrete* — especially for relatively intact (uncracked) pavements.
4. *Compressive stresses or strains at the top of the unbound materials* — when the failure mechanism is likely to be something other than reflective or fatigue cracking (e.g. roughness).

However to correctly develop fatigue transfer functions between laboratory results and field observations, it is necessary that test are executed under appropriate loading conditions.

Traditionally, flexural fatigue tests have been executed either under controlled stress or controlled strain, in an attempt to capture loading conditions similar to those encountered in the field. In controlled stress tests, the amplitude of the load is held constant while the displacement of the specimen increases as the damage increases. When this test is properly executed, there are mechanisms that prevent the test specimen from returning to its original position after each load cycle. This causes the accumulation of permanent deformation. Conversely, in controlled strain tests the amplitude of the displacement is maintained constant while the load needed to cause that displacement is reduced as the damage increases. For reflective cracking fatigue tests, similar considerations have been used to obtain an indication of actual fatigue life. The key questions that need to be address are: (1) under which conditions should one mode of loading or another be used in the laboratory, and (2) could any other combination of these modes be used? These two questions are addressed separately for the reflective cracking and for the flexural cracking analyses in the following sections.

All the analyses presented were done under the assumption that all pavement distress in the form of cracking starts with microcracks. As such, it is fairly clear that the overall pavement stiffness (or effective "modulus") generally decreases under fatigue loadings, either for the AC pavement layer (in flexural fatigue) or above the crack zone (in reflective cracking). In each case, assuming a reduced modulus for the zone or layer subject to fatigue simulates the evolution of damage. It is also clear that thin overlays placed over cracked pavement sections rapidly exhibit a crack pattern identical to that of the original cracked pavement.

2. Reflective Cracking Analysis

Several types of test have been used to simulate the reflective cracking phenomena (Brown et.al., 1989; Francken, 1993; de Bondt, 1995; di Benedetto et.al., 1993; Vecoven, 1989). However, no clear indication has been forthcoming regarding the correct mode of loading to best simulate field conditions. The complexity of the loading mechanism in reflective cracking together with temperature stresses may mask their main effects.

The modeling approach followed herein attempts to determine which parameters (stress, displacement, strain, or work) remain mostly constant in the field, as reflective cracking progresses and as the material becomes damaged and weakens above a crack.

In this analysis, it is assumed that the relative displacement between points A and B in the actual phenomenon when a crack develops will be the same as the relative displacement between points A1 and B1 in the computer simulated phenomenon, as shown in *Figure 1*.

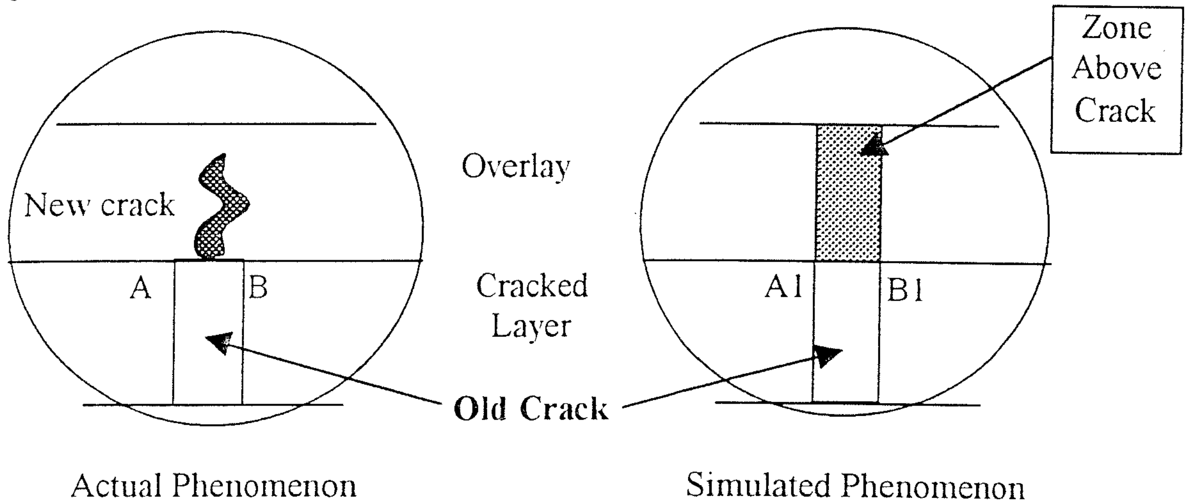

Figure 1: Modeling Idealization

It can be shown that there are levels of stiffness or modulus that can be selected for the zone above the crack that simulate actual crack propagation. It is, however, not so easily justified that the stress near the crack, as it develops, is identical to that inside a uniform zone modeled by a uniform modulus in the zone above the crack. However, the important aspect to be considered is how the overall evolution of stresses near the crack develop as the modulus decrease to insure the compatibility of the boundary value solution.

2.1 Modeling

For this study, the SAP2000 finite element program was used as the modeling tool. The linear elastic ASOLID element under the plain strain mode was used in the analyses. A mesh with 1920 elements was used to model the subgrade layer, the base layer, the cracked bituminous layer, the overlay, the crack and the zone above the crack, as show in *Figure 2*. A 65 kN dual tire load was applied immediately to the left of the crack, assuming that it would be applied over a length of one meter. The analyses simulated the stresses near a longitudinal crack, since Pais (1999) identified that longitudinal cracks are the most critical with respect to the onset of reflective cracking.

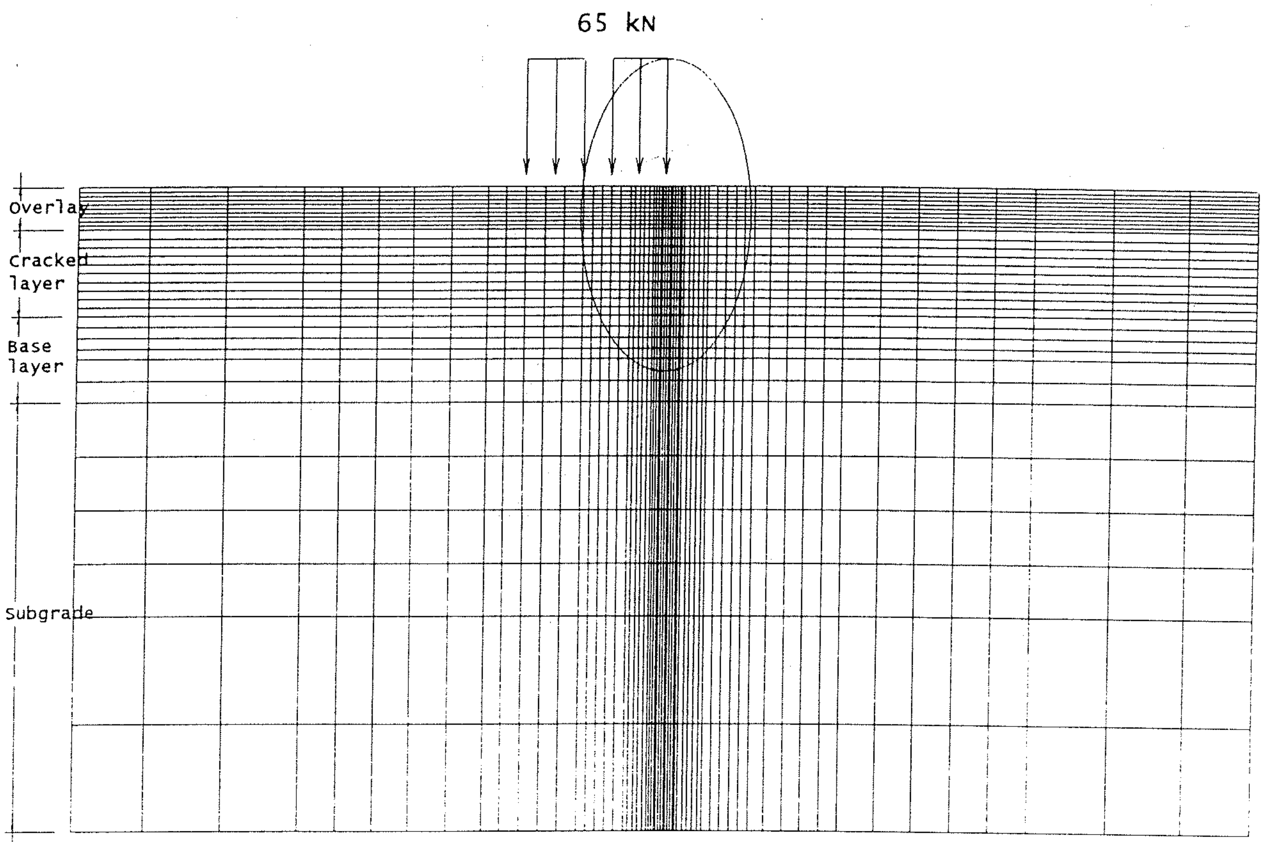

Figure 2: Overall Mesh (Vertically Distorted to Show Elements)

It is recognized that a 3D model should be used if an exact analysis of stresses and strains are required (for instance in the case of modeling an actual pavement section). However for the purpose of these analyses, the precise stress or strain values levels are not required — only the *relative* stress and strain values between the modulus levels used in the analyses.

To model the existing crack, 3 x 10 = 30 elements were assigned a very low stiffness (1 MPa, see *Figure 3*). The 3 x 10 elements above the crack were assigned varying moduli, thus simulating the effect of microcracks. The assigned modulus levels for the elements above the crack were: 4500, 3500, 2500, 1500, 500 and 100 MPa.

2.2 Cases Investigated

To broaden the analysis, several situations were modeled to investigate the relative effect of some of the variables known to affect cracked pavement overlay performance, such as crack width, overlay modulus, cracked layer modulus and overlay thickness. Since the subgrade has little influence on reflective cracking, its modulus was maintained constant at 60 MPa. The crack widths evaluated were 5, 10 and 15 mm, corresponding to three typical crack widths found in the field, as proposed by Pais (1999).

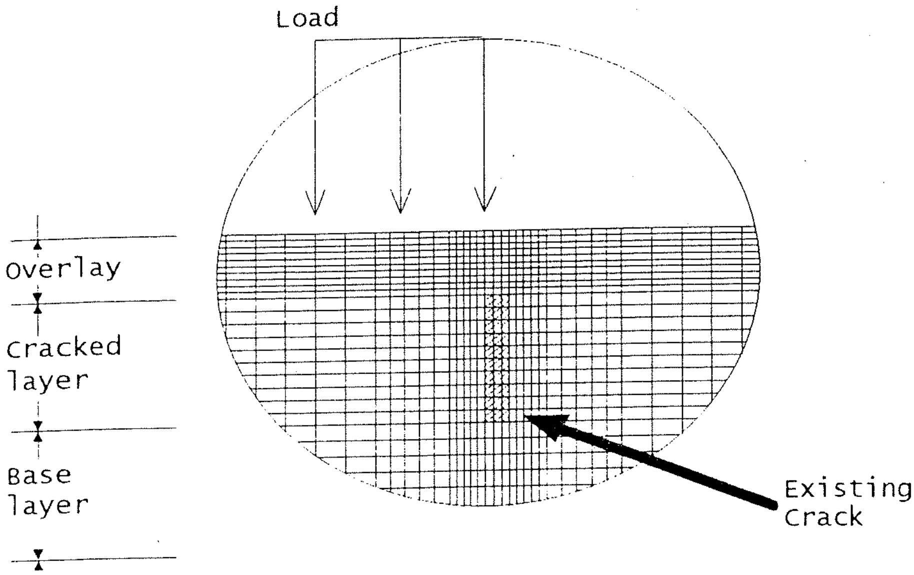

Figure 3: Detail of a Crack Modeled With 30 (3 x 10) Elements

The overall stiffness, or modulus, of the cracked layer was varied between 2000 MPa and 3500 MPa. These are values typically found through backcalculation of flexible pavement surface layers when an overlay is needed. The overlay thickness was varied between 40, 80 and 120 mm. The thickness of the exiting cracked pavement layer was varied between 150, 200 and 250 mm. A total of 324 simulations were computed.

A "Set" is defined as a series of cases in which the stiffness above the crack zone is decreased from 4500 to 100 MPa using the incremental steps proposed above. As such, a total of 54 Sets were studied in an attempt to simulate the evolution of stresses and strains that affect the crack zone as the modulus of the material above the crack is reduced through microcracking.

2.3 Analysis and Results

To analyze this massive amount of data, a software program was written to extract the needed information. Specifically, for each case the relative displacement of the crack tips was extracted, namely (Δx and Δy) along with the average stresses and strains in the three center elements in the zone above the crack. It has been shown that greater stress concentrations are found in the zone above the crack, as can be seen in *Figure 4* which represents the so-called "Von Mises" stresses.

The average stress and strain in the X, Y and XY directions were then computed. X corresponds to the horizontal direction, Y corresponds to the vertical direction, and XY corresponds to the shear component. The average work done was determined by multiplying the average stress by the average strain. The software then grouped the extracted data for each Set. Typical results can be observed in the examples shown in *Figures 5 and 6*, for a 50 mm overlay thickness, a 150 mm cracked layer thickness, and a 2000 MPa cracked layer modulus.

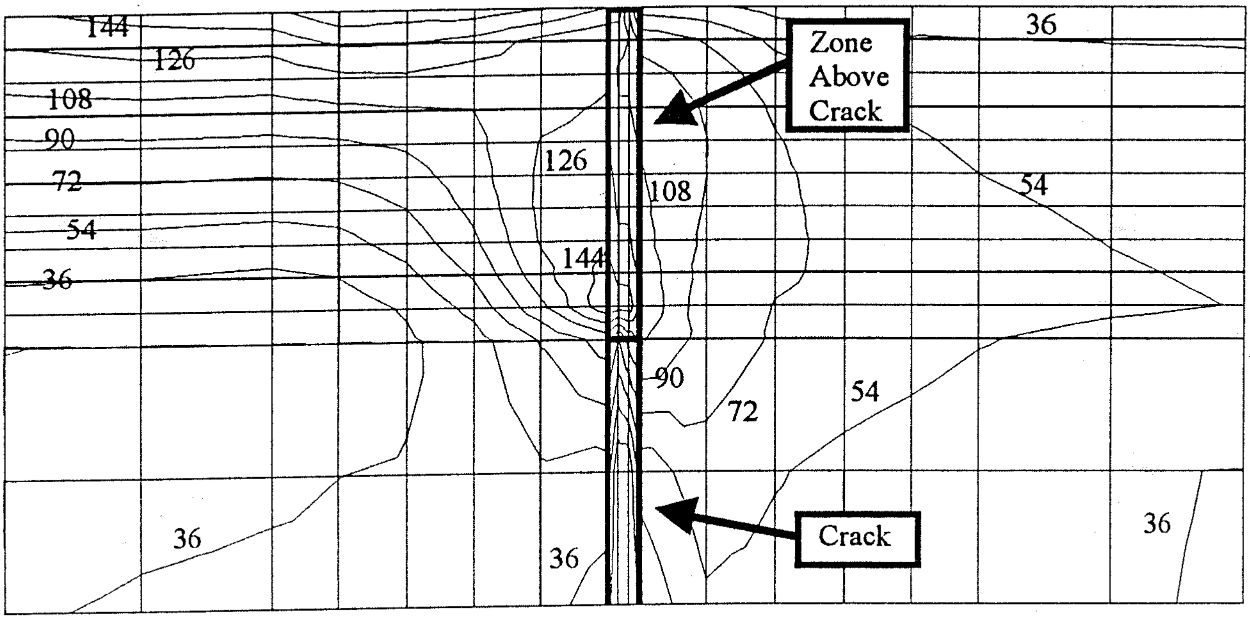

Figure 4: Von Mises Stresses Near the Crack Zone (kPa)

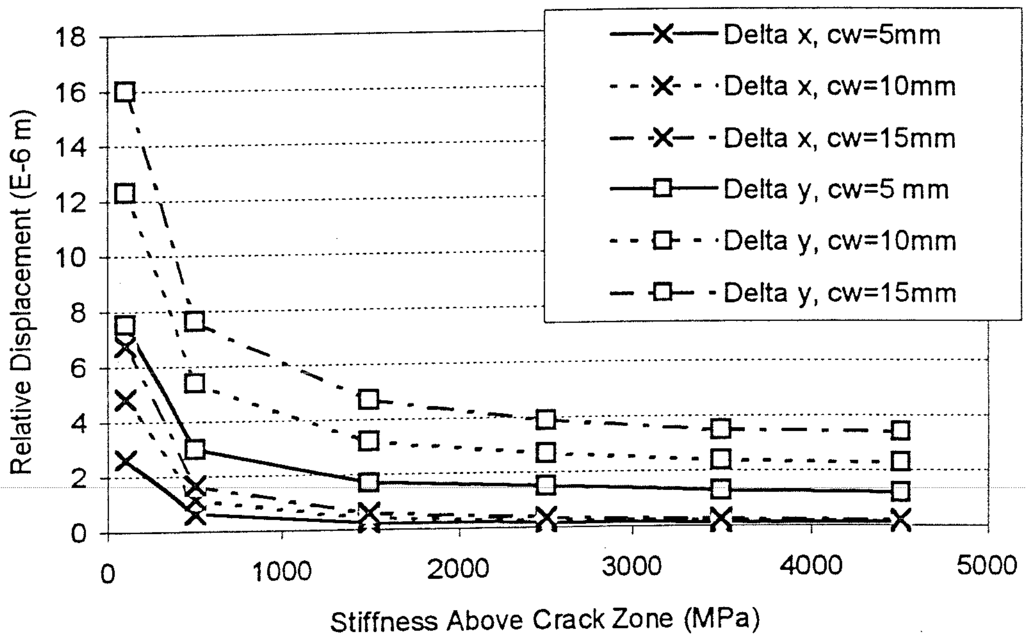

Figure 5: Variation in the Relative Displacement of the Crack Tip with Stiffness Above the Crack Zone

It can be observed in *Figure 6* that as the modulus of the material above the crack decreases, the stresses remain relatively constant within the crack zone. Meanwhile, it can be observed in *Figure 5* that the relative displacement of the crack increases as the modulus in the crack zone decreases.

For each Set studied, the ratios between the stress, strain, work and displacement values obtained in the case where the modulus above the crack zone was 4500 MPa were divided by the same values as the modulus was first reduced to 2500 MPa and then to 100 MPa. If the ratios decreased, the inverse of the ratio was calculated.

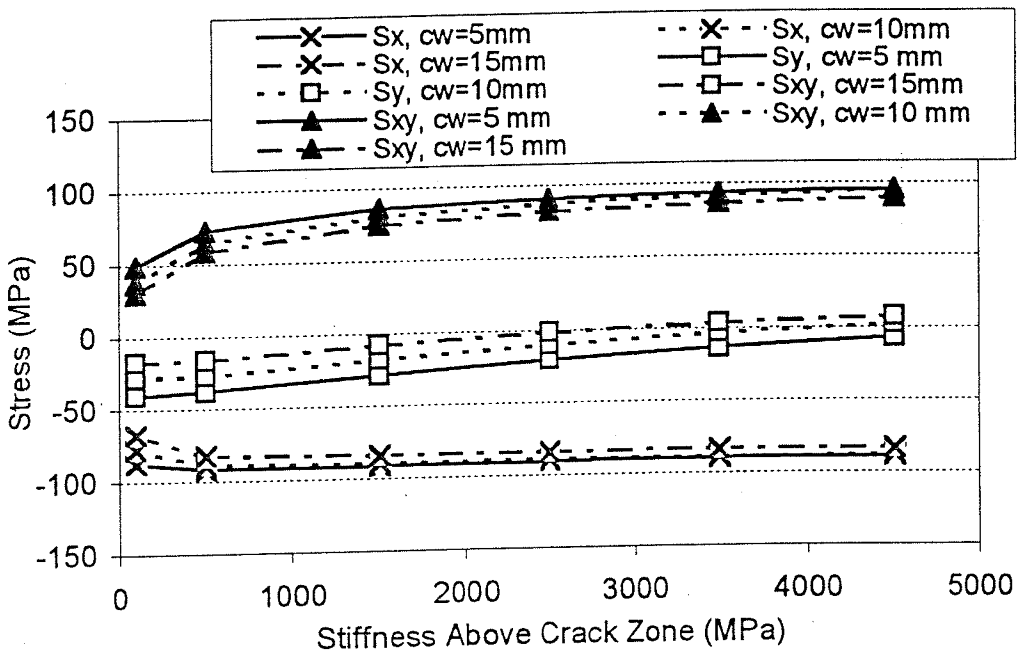

Figure 6: Variation of Stresses With Stiffness Above Crack Zone

The ratio to 2500 MPa was based on the rational that laboratory fatigue displacement control tests are generally executed until the modulus is reduced to 50% of its initial value.

To illustrate, *Table 1* presents the numerical ratios for a crack width of 5 mm obtained for a change in modulus from 4500 to 2500 MPa, while *Table 2* shows the corresponding ratios for a change in modulus from 4500 MPa to 100 MPa. Similar values were obtained for the other investigated crack widths. In the *Tables 1 and 2*, "OT" represents the overlay thickness. "BT" represents the cracked layer thickness and "BS" represents the cracked layer stiffness or modulus.

On the bottom of each table, the averages of all the computed ratios are presented. It can clearly be concluded that the two parameters that show the least change as the crack propagates are the average shear stress, XY, in the center elements and the average compressive stress, X. In general, the magnitude of all other parameters evaluated show a greater degree of change as the stiffness above the crack zone decreases.

Based on these results, it is apparent that the reflective cracking phenomenon is best simulated in the laboratory by utilizing a combined controlled shear and tensile/compressive stress testing protocol. From these analyses, however, it is not clear what the exact magnitude of those stresses should be, as the plain strain simulation does not permit that determination with an adequate degree of accuracy. Furthermore, the tensile stress levels may also be affected, to some degree, by thermal stresses in the pavement that have not been considered in this analysis.

Table 1: Ratios between 4500 MPa and 2500 MPa for Reflective Cracking

OT	BT	BS	Ratios										
(mm)	(mm)	(MPa)	δx	δy	σx	σy	σxy	εx	εy	εxy	ωx	ωy	ωxy
40	0.15	2000	1.53	1.25	1.02	2.86	1.05	1.68	1.24	1.72	1.71	3.55	1.65
40	0.15	3500	1.48	1.25	1.03	4.69	1.05	1.68	1.24	1.71	1.73	5.82	1.62
40	200	2000	1.49	1.25	1.03	2.41	1.05	1.70	1.26	1.72	1.75	3.04	1.65
40	200	3500	1.45	1.25	1.04	2.78	1.05	1.72	1.27	1.71	1.78	3.52	1.62
40	250	2000	1.47	1.25	1.03	2.10	1.05	1.72	1.28	1.72	1.78	2.69	1.65
40	250	3500	1.43	1.28	1.05	2.17	1.05	1.75	1.29	1.71	1.83	2.81	1.62
80	150	2000	1.48	1.11	1.03	17.75	1.00	1.57	1.13	1.80	1.52	20.11	1.81
80	150	3500	1.45	1.22	1.04	1.61	1.00	1.52	1.12	1.81	1.46	1.44	1.82
80	200	2000	1.32	1.25	1.01	5.15	1.00	1.61	1.14	1.81	1.59	5.88	1.82
80	200	3500	2.40	1.26	1.01	4.51	1.01	1.59	1.13	1.81	1.57	5.09	1.83
80	250	2000	1.68	1.27	1.00	2.82	1.01	1.64	1.15	1.81	1.64	3.24	1.83
80	250	3500	1.56	1.28	1.01	5.62	1.01	1.64	1.14	1.82	1.66	6.42	1.83
120	150	2000	1.57	1.14	1.19	5.86	1.02	1.36	1.12	1.83	1.14	5.21	1.87
120	150	3500	1.56	1.16	1.15	3.58	1.03	1.36	1.09	1.85	1.18	3.28	1.90
120	200	2000	1.57	1.27	1.07	2.16	1.02	1.51	1.12	1.84	1.41	2.42	1.89
120	200	3500	1.55	1.28	1.07	3.21	1.03	1.47	1.09	1.86	1.38	2.93	1.92
120	250	2000	1.56	1.27	1.04	6.09	1.03	1.57	1.12	1.85	1.51	6.82	1.90
120	250	3500	1.53	1.32	1.03	2.73	1.04	1.54	1.10	1.87	1.50	3.00	1.93
		Avg:	1.55	1.22	**1.06**	4.33	**1.06**	1.61	1.17	1.78	1.55	4.83	1.78

It can also be concluded that previously reported reflective crack tests conducted by Sousa et.al. (1996) and by Pais (1999), where displacements were imposed in the Reflective Cracking Device (RCD), do not truly represent the reflective cracking phenomena in the field, because the RCD displacements appeared to increase as the crack propagated. Simultaneously, the material stiffness above the crack became weakened by microcracking.

Nevertheless, if material performance comparisons are made down to a 50% modulus reduction level only, the original results are at least a first order approximation of the "truth". This is because the changes in relative displacements in the crack tip as the modulus falls from 4500 to 2500 MPa are not very large, as was shown in *Figure 5*. The average values in *Table 1* also demonstrate that the ratios in the X and Y displacement directions are closer to the ratios obtained from the combined tensile and shear stress loading combination.

Table 2: Ratios Between 4500 MPa and 100 MPa for Reflective Cracking

OT	BT	BS	Ratios										
(mm)	(mm)	(MPa)	δx	δy	σx	σy	σxy	εx	εy	εxy	ωx	ωy	ωxy
40	0.15	2000	22.87	6.25	1.01	5.66	1.96	34.88	6.88	22.96	34.42	38.93	11.72
40	0.15	3500	18.11	6.42	1.04	9.88	2.19	33.24	6.30	20.59	31.86	62.18	9.42
40	200	2000	18.58	7.00	1.04	4.37	1.94	34.48	7.26	23.15	33.19	31.72	11.91
40	200	3500	14.46	7.08	1.07	5.03	2.18	33.24	6.91	20.68	31.11	34.77	9.51
40	250	2000	16.05	7.51	1.06	3.52	1.94	34.39	7.69	23.26	32.57	27.08	12.02
40	250	3500	12.45	7.28	1.08	3.50	2.17	33.49	7.55	20.72	30.92	26.45	9.54
80	150	2000	12.02	6.33	1.29	66.62	1.48	41.76	2.24	30.48	53.89	149.09	20.64
80	150	3500	15.27	6.56	1.16	4.03	1.57	35.18	1.93	28.64	40.93	7.75	18.23
80	200	2000	73.04	7.62	1.19	14.36	1.47	39.61	2.67	30.70	47.01	38.41	20.95
80	200	3500	274.0	7.13	1.11	14.88	1.57	35.67	2.43	28.74	39.72	36.10	18.36
80	250	2000	63.56	7.75	1.14	6.49	1.46	39.13	3.05	30.88	44.63	19.80	21.19
80	250	3500	28.56	7.59	1.10	13.66	1.56	36.77	2.90	28.81	40.42	39.56	18.44
120	150	2000	5.24	6.86	1.86	3.93	1.28	52.39	8.61	35.17	97.39	2.19	27.49
120	150	3500	3.07	6.99	1.19	1.42	1.33	31.09	1.44	33.96	37.03	1.01	25.62
120	200	2000	1.94	7.89	1.36	11.81	1.27	42.40	1.09	35.48	57.56	12.83	27.97
120	200	3500	1.43	7.69	1.11	3.02	1.32	32.72	1.16	34.16	36.47	3.50	25.93
120	250	2000	3.97	8.14	1.23	19.00	1.26	40.47	1.53	35.74	49.76	29.12	28.38
120	250	3500	14.09	8.11	1.10	9.91	1.31	34.65	1.50	34.32	38.17	14.88	26.17
		Avg:	33.3	7.22	**1.17**	11.2	**1.61**	37.0	4.06	28.8	43.2	31.9	19.1

3. Flexural Fatigue Analysis

3.1 Modeling

The ELSYM program was used to model the pavement structure in this analysis. A standard flexible pavement structure was modeled, composed of a subgrade layer, a granular base layer, and an asphalt concrete layer. A dual wheel load of 65 kN was applied to the pavement surface. Typical values of Poisson's ratio were used for each structural layer. The resulting tensile stress and strain at the bottom of the asphalt concrete layer was then computed. The product of the stress time the strain was deemed to be a good measure of elastic energy, or "work".

To simulate the evolution of tensile stresses, strains, and work at the bottom of the AC layer as its modulus decreases through microcracking, the modulus of the AC layer was modeled to decrease from a starting value of 5000 MPa down to 1000 MPa, in 500 MPa increments. The lower value of 1000 MPa is based on the consideration that AC layers are rarely found with moduli lower then that value.

3.2 Cases Investigated

Four AC pavement layer thicknesses were investigated: 250, 200, 150 and 100 mm. For each thickness, three subgrade moduli were considered: 50, 100 and 150 MPa. The base modulus was maintained constant at 250 MPa.

A total of 108 cases were computed. A "Set" is defined as a group of cases where the evolution of the moduli varied step-wise downward, from 5000, to 4500, 4000, 3500, 3000, 2500, 2000, 1500 and finally 1000 MPa. A total of 12 Sets were considered in the analyses.

3.3 Analysis and Results

A software program was written to extract the required data from each case, grouping them in the appropriate output sets. The required values of stress, strain and work were computed and then plotted against the AC moduli. The variation in tensile stresses and work is shown in *Figures 7 and 8*, respectively, as the modulus is reduced.

It can be observed that in thick pavements, the computed stress remains mostly constant. For thin pavements, more variation is noted (see *Figure 7*). However it can be observed that the <u>*product*</u> of stress and strain (i.e. work) remains mostly constant for both the thick and thin pavements.

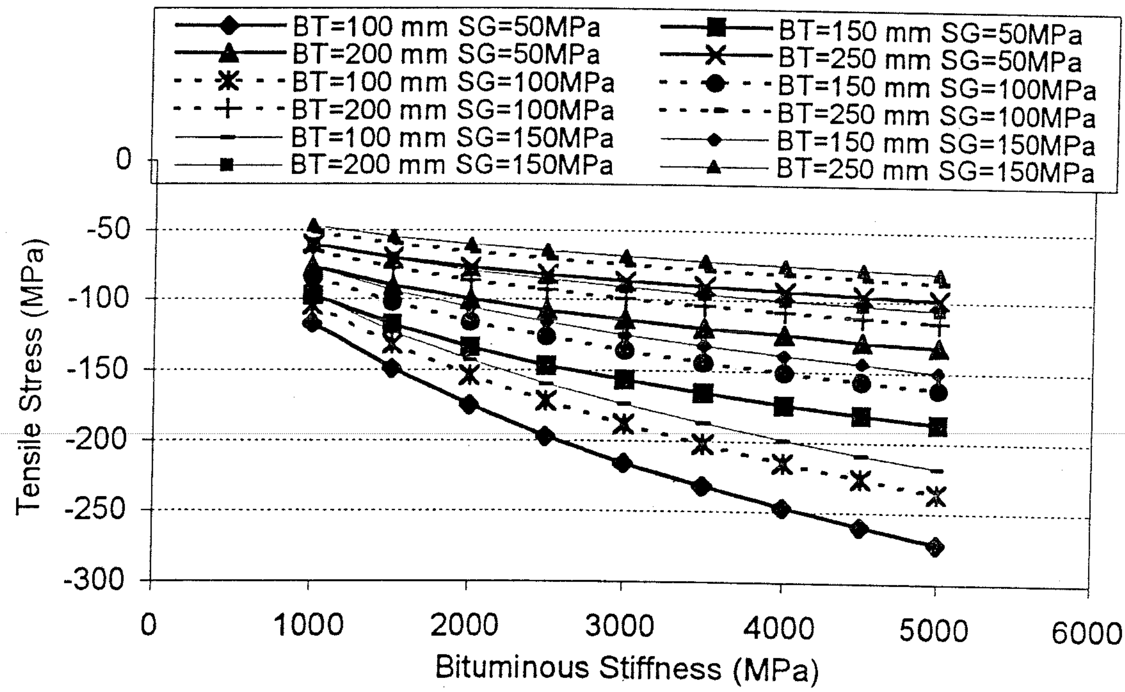

Figure 7: Variation of Tensile Stress With AC Layer Stiffness

The ratio of the stress, strain and work at 5000 MPa to the same values at 2500 and 1000 MPa, respectively, were computed for each case and are presented in *Tables 3 and 4*.

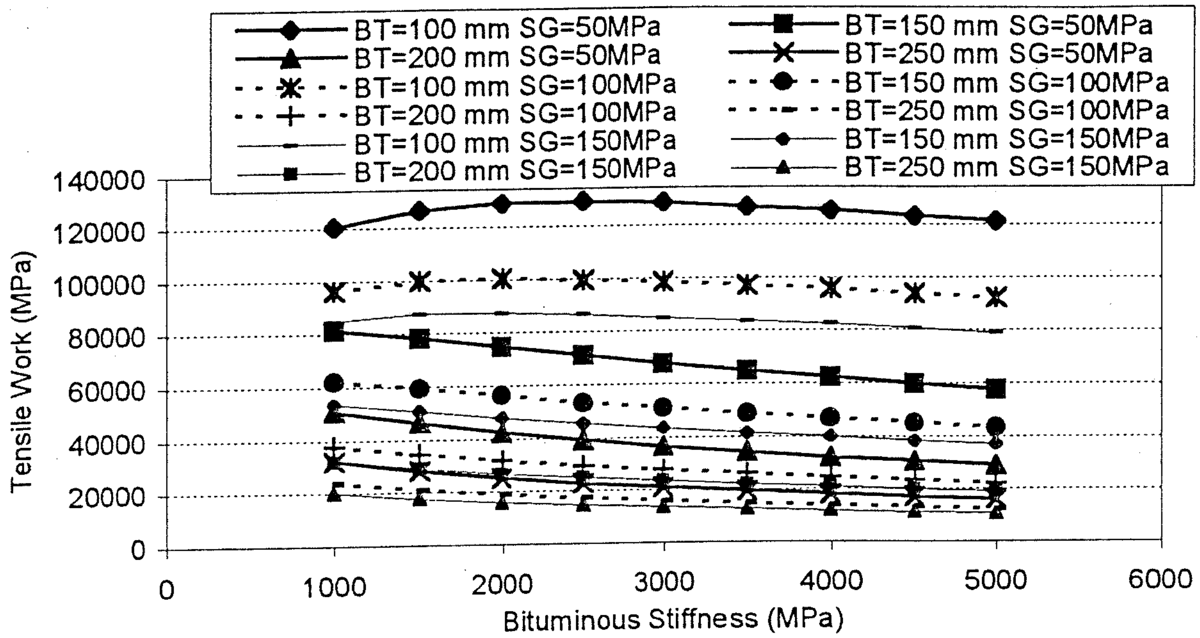

Figure 8: Variation of Tensile Work With AC Layer Stiffness

Table 3: Ratios Between 5000 and 2500 MPa for Flexural Fatigue

Bituminous Thickness (mm)	Subgrade Moduli (MPa)	Ratios		
		Strain	Stress	Work
100	50	1.47	1.38	1.07
150	50	1.58	1.27	1.24
200	50	1.66	1.22	1.36
250	50	1.70	1.20	1.42
100	100	1.48	1.37	1.08
150	100	1.58	1.29	1.23
200	100	1.65	1.23	1.33
250	100	1.70	1.21	1.40
100	150	1.49	1.36	1.10
150	150	1.59	1.29	1.23
200	150	1.64	1.24	1.32
250	150	1.68	1.23	1.37
	AVERAGE:	**1.60**	**1.27**	**1.26**

From the average values computed and shown at the bottom of *Tables 3 and 4,* it can be concluded that the product of stress times strain (= work) remains mostly constant in the flexural fatigue mode simulation. As such, it would appear that flexural fatigue tests should generally be executed in the controlled (constant) work mode. In such cases, the product of the amplitude of the force times the amplitude of the displacement should remain constant as the flexural fatigue test progresses. However, it is clear from the data that relative comparisons of performance for thicker pavements could also be executed under controlled stress as long as the test is terminated when the reduction in modulus reaches 50% of its initial value.

Table 4: Ratios Between 5000 MPa and 1000 MPa for Flexural Fatigue

Bituminous Thickness	Subgrade Moduli	Ratios		
(mm)	(MPa)	Strain	Stress	Work
100	50	2.31	2.32	0.99
150	50	2.73	1.93	1.42
200	50	3.03	1.72	1.76
250	50	3.27	1.63	2.01
100	100	2.37	2.27	1.05
150	100	2.77	1.93	1.44
200	100	3.00	1.76	1.71
250	100	3.23	1.68	1.93
100	150	2.41	2.24	1.08
150	150	2.79	1.93	1.45
200	150	2.97	1.77	1.68
250	150	3.18	1.70	1.87
	AVERAGE:	**2.84**	**1.91**	**1.53**

4. Conclusions and Recommendations

This paper presents a numerical computer analysis, using a finite element approach, that investigates the predominant mode of loading in reflective cracking and flexural fatigue phenomena in AC pavements. Plain strain analysis was executed using the SAP2000 program to simulate the state of stress and strain adjacent to a longitudinal pavement crack. The ELSYM program was used to simulate the state of stress and strain at the bottom of the AC layer for an uncracked pavement.

Reducing the modulus either in the zone above the crack (reflective fatigue) or in the overall AC layer (flexural fatigue) were the mechanisms used to simulate the effect of accumulated damage from cracking.

From the analyses presented in this paper and within the set of data studied, it can be concluded the reflective cracking phenomena is best simulated in the laboratory by executing tests under controlled stress by applying a combination of shear and tensile/compressive stresses. Flexural fatigue tests, on the other hand, should be executed under controlled "work" (stress times strain) by keeping the product of the load times the displacement imposed to the specimen constant. However, controlled stress tests are also adequate for relative performance comparisons as long as they are only carried out until the modulus of the specimen decreases by 50%.

5. References

1. Brown, S.F., J.M. Brunton & R.J. Armitage. 1989. *Grid reinforced overlays*. Proceedings of the First International RILEM Conference on Reflective Cracking in Pavements.

2. Francken, L., 1993. *Laboratory Simulation and Modeling of Overlay Systems*. Proceedings of the Second International RILEM Conference on Reflective Cracking in Pavements.

3. de Bondt, A.H., 1995. *Theoretical Analysis of Reinforcement Pullout*. Report 7-95-203-16, Road and Railroad Research Laboratory, Delft University of Technology.

4. di Benedetto, H., J. Neji, J.P. Antoine & M. Pasquier, 1993. *Apparatus for laboratory study of cracking resistance*. Proceedings of the Second International RILEM Conference on Reflective Cracking in Pavements.

5. Vecoven, J.H., 1989. *Methode d'etude de systèmes limitant la remontée de fissures dans les chaussées*. Proceedings of the First International RILEM Conference on Reflective Cracking in Pavements.

6. Pais, J.P., 1999. The Reflective Cracking in Flexible Pavement Overlay Design. Ph.D. Thesis, University of Minho, Portugal.

7. Sousa, J.B., S. Shatnawi, & J. Cox, 1996. *An approach for investigating reflective fatigue cracking in asphalt-aggregate overlays*. Proceedings of the Third International RILEM Conference on Reflective Cracking in Pavements.